Cellulose (2019) 26:8813–8827
https://doi.org/10.1007/s10570-019-02673-w

ORIGINAL RESEARCH

Effects of cellulose nanofibrils on dialdehyde carboxymethyl cellulose based dual responsive self-healing hydrogel

Ying Wang · Guifa Xiao · Yangyang Peng · Liheng Chen · Shiyu Fu

Received: 27 April 2019 / Accepted: 9 August 2019 / Published online: 21 August 2019

Abstract A self-healing hydrogel containing acylhydrazone bond and disulfide bond with pH and redox dual responses was prepared by crosslinking dialdehyde carboxymethyl cellulose (DCMC) with 3,3′-dithiobis(propionohydrazide) (DTP). The pH, gelator concentration and oxidation degree of DCMC affected the formation of DCMC-based self-healing hydrogels seriously. Interestingly, addition of cellulose nanofibers (CNFs) improved the mechanical property of the DCMC-based self-healing hydrogel and its efficiency. When 1.0 wt% CNFs was added in hydrogel preparation, the compressive strength (1.05 MPa) of the composite hydrogel increased by 275% and its strain rose to 74.6%. The healing rate of hydrogel containing 1.0 wt% CNFs was 82.7% at 0.5 h and 89.9% at 1 h, which was much faster than that of original hydrogel (51.6% at 0.5 h and 58.5% in 1 h). DCMC-based dual responsive self-healing hydrogel showed good biocompatibility confirmed by cytotoxicity test, which is potential to implement in medial field.

Y. Wang · G. Xiao · Y. Peng · S. Fu (✉)
State Key Laboratory of Pulp and Paper Engineering, South China University of Technology, Guangzhou 510640, China
e-mail: shyfu@scut.edu.cn

L. Chen
Key Laboratory of Biomaterials of Guangdong Higher Education Institutes, Department of Biomedical Engineering, Jinan University, Guangzhou 510632, China

Graphic abstract

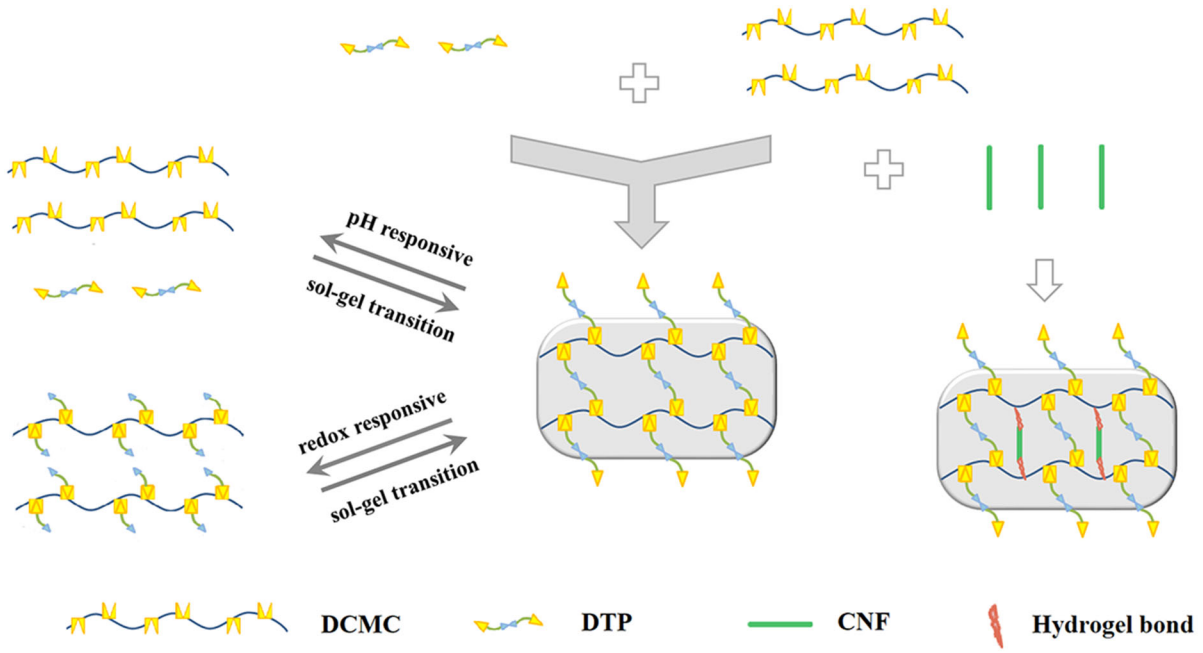

Keywords Dialdehyde carboxymethyl cellulose · Hydrogel · Self-healing · Dual responses · Cellulose nanofibers

Introduction

Hydrogels with three-dimensional cross-linking network structure are acknowledged to absorb and maintain a large amount of water but cannot dissolve themselves (Hussain et al. 2018a). In recent years, hydrogels have been extensively explored and applied in various fields due to their strong hydrophilicity, low friction coefficient and environmental sensitivity properties, such as drug-controlled release (Chen et al. 2018), tissue engineering (Yu et al. 2014), sensors (Maity et al. 2018), etc. However, conventional hydrogels often suffer from poor mechanical properties and are easy to deform or be damaged when subjected to mechanical forces. The accumulation of hydrogel damage would affect its integrity and result in loss of the functionalities and limit of lifespan. Therefore, it is desirable to develop robust hydrogels with self-healing capability, which can not only prolong the service life of materials, but also avoid the accumulation of cracks or damage and improve the durability and reliability of hydrogels in certain applications (Wang et al. 2018b).

Nowadays, the preparation of self-healing hydrogels is mainly based on dynamic chemistry, including non-covalent chemistry and dynamic covalent chemistry (Liu et al. 2016). Common dynamic covalent bond such as phenylboronic esters (Xu et al. 2011), Diels–Alder reactions (Yu et al. 2015) and imine bonds (Zhu et al. 2017), which are usually based on complex synthetic procedures, and need additional stimuli to trigger the self-healing process. Acylhydrazone bond, a dynamic covalent bond obtained by condensation reaction of aldehyde group with hydrazide, has mild reaction conditions and good biocompatibility for designing self-healing hydrogels (Wei et al. 2015). Disulfide bond is another attractive dynamic covalent bond which has good biocompatibility and often used to prepare self-healing hydrogels (Guo et al. 2017). Disulfide bond is a covalent bond sensitive to redox and easy to break into sulfhydryl group under reduction condition, and regenerate under oxidation condition (Yang et al. 2018b). In addition, acylhydrazone and disulfide bond exchange reactions were proved to be compatible and can react independently upon pH in a single system of solvents (Deng

et al. 2012). Therefore, it would be interesting to obtain a complex system with controllable responsiveness by the incorporation of the two dynamic bonds into the same network. To integrate these two bonds into the same network Carboxymethyl cellulose (CMC) was oxidized by periodate to break the C2–C3 bond of 1,4-glucan unit and convert hydroxy groups into paired aldehydes with high specificity to form dialdehyde carboxymethyl cellulose (DCMC). The agent 3,3′-dithiobis(propionohydrazide) (DTP) were prepared to form dynamic acylhydrazone bond and provide disulfide bond.

Excellent mechanical properties of self-healing hydrogels are the prerequisite for their practical application to achieve high and stable performance under repeated deformation state. Sophisticated design of 3D network structure is a common/traditional method to improve the strength of hydrogel. Recently, the introduction of sacrificial bond has become another popular method to design hydrogels with high mechanical properties (Hussain et al. 2018b; Yang et al. 2013, 2018a). The breakage of weak bonds under stress dissipates energy, which results in toughness of hydrogels (Hussain et al. 2018b). Cellulose nanofibers (CNFs), a natural polysaccharide with natural crystal structure have become environmentally friendly reinforcement particles due to their excellent mechanical properties, renewability, biocompatibility, biodegradability and abundant surface (Abe and Yano 2012; Li et al. 2016). Liu et al. added only 0.05 wt% cellulose nanocrystals (CNCs) to the covalently crosslinked homogeneous polymer networks and the tensile stress and breaking elongation of hydrogels increased from 0.5 to 1.0 MPa, from 700 to 1160%, respectively (Liu et al. 2017b). Liu et al. added amino modified cellulose nanocrystals when cellulose acetate (CAA) crosslinked with hydroxypropyl chitosan (HPCS). The elastic modulus of hydrogels increased by 150% (Liu et al. 2018).

In this work, the self-healing hydrogels containing acylhydrazone bond and disulfide bond were prepared from DCMC with dialdehyde and crosslinking agent DTP containing hydrazide group and disulfide bond. The effects of CNFs on the mechanical properties, sol–gel and self-healing properties of hydrogel were studied.

Experimental part

Materials

Sodium carboxymethyl cellulose, sodium periodate, hydroxylamine hydrochloride and hydrazinium hydrate (80% in water) were purchased from aladdin Industrial Corporation and dimethyl 3,3′-dithiodipropionate was purchased from Shanghai McLean biochemical technology CO., LTD. Bamboo pulp was supplied by Yibin paper industry CO., LTD, Sichuan China. Other solvents were analytical grade and used as received without any purification. Deionized water was used throughout the experiments.

Methods and procedures

Preparation of DCMC

The preparation of DCMC was referred to previous literatures (Li et al. 2011; Tian and Jiang 2018) with certain modifications. The uniform and transparent CMC solution was obtained by adding 15 g CMC into 800 mL water with stirring at room temperature for 12 h. 200 mL sodium periodate solution was added to the above-mentioned solution and the pH was adjusted to 3.0–3.5 with sulfuric acid at 40 °C in darkness. Excessive ethylene glycol was added and reacted for another 1 h to stop the reaction. The oxidized product was dialyzed against deionized water to remove unreacted reagents and by-products and stored at 4 °C. The aldehyde group contents (A) of DCMCs were calculated according to Eq. (1) according to the method in literature (Li et al. 2011) and the results were listed in Table 1.

$$A(\%) = \frac{c_{\mathrm{NaOH}} \cdot (V_2 - V_1)}{m/211} \times 100 \quad (1)$$

where, c_{NaOH} denotes the concentration of NaOH, mol/L; V_1 denotes the amount of NaOH consumed by CMC, mL; V_2 denotes the amount of NaOH consumed by DCMC, mL;m is the oven weight of DCMC, g. 211 represents the average approximate relative molecular mass of the repeating unit CMC and DCMC. Each sample was tested in parallel for three times and the result error was no more than 1%, and then the average value was taken.

Table 1 Reaction conditions and number average molecular weight of DCMC with different oxidation degrees

DCMC	n($NaIO_4$): n(CMC)	reaction time (h)	oxidation degree (%)	Mn (g mol^{-1})
O_{11}	0.5:1.0	1	11.4 ± 0.75	1.1×10^6
O_{19}	1.0:1.0	2	19.4 ± 0.80	6.1×10^5
O_{27}	1.0:1.5	2	27.2 ± 1.14	3.7×10^5

Preparation of cross-linking agent

DTP was prepared according to the literature (Rodriguez-Docampo and Otto 2008). Briefly, 10 g 3, 3′-dithiodimalonate dimethyl ester was dissolved in 300 mL absolute methanol, and 100 mL hydrazine hydrate was added. The mixture was stirred at room temperature for 12 h. Decompression filtration was performed after stirring in ice-water bath for 1 h, successively followed washing with 100 mL cold methanol, 20 mL water and 50 mL cold methanol to obtain a white solid.

Preparation of CNFs

Cellulose nanofibrils (CNFs) were prepared according to our previously reported method (Peng et al. 2019). Bamboo pulp was hydrolyzed by 57 wt% H_2SO_4 at 45 °C for 40 min under continuous mechanical stirring. The obtained suspension was immediately diluted six-fold deionized water to terminate reaction. The CNFs in the sediments were washed with water to remove excessive acid by centrifugation at 5500 rpm for 10 min three times and then dispersed in water. Sodium hydroxide solution was to neutralize residual acid. The salt was removed by two centrifugations. Finally, the suspension was homogenized under 800 bar at room temperature by Nano micro jet homogenizer MINI to obtain a uniform CNFs dispersion before stored at 4 °C. Some of them were freeze-dried for further experiment.

Preparation of hydrogels

Hydrogel was obtained by briefly mixing DCMCs solution with DTP solution at ambient temperature and their pH values were adjusted by adding NaOH or H_2SO_4 solution. The molar ratio of aldehyde group to acylhydrazine group was kept at 1:1. The freeze-dried CNFs of different molar ratio was added to DCMCs solution and stirred for 12 h to form a uniform mixture. The mixture was sonicated for 2 min before mixed with DTP solution and the CNFs composited hydrogels were obtained. In the hydrogel, gelator concentration is the rate of DCMC and DTP in weight to the whole hydrogel. Except the experiment to explore the effect of gelator concentration on formation of self-healing hydrogel, the gelator concentration was 8% for other hydrogel preparations.

Characterization methods

Gel permeation chromatography (GPC)

The molecular weight of DCMCs was determined by a water-based GPC system (Waters, USA). DCMCs were dissolved in a mobile phase with a final concentration of 2–3 mg/mL and filtered by a 0.45 μm drainage membrane with an injection volume of 10 μL. The running time was 45 min, and the chromatogram was recorded. The chromatographic conditions included the 0.02 mol/L KH_2PO_4 buffer solution mobile phase, TSK G-5000PWXL column (7.8 × 300 mm) and TSK G-3000PWXL column (7.8 × 300 mm) in series. The flow rate was 0.6 mL/min, and the column temperature was 35 °C.

Fourier transform infrared spectroscopy (FTIR) analysis

The characteristic functional groups of CMC, DCMC and hydrogel were analysed with an IR Thermo Fisher Scientific Nicolet 6700 spectrometer between 500 and 4000 cm^{-1}.

Nuclear magnetic resonance (NMR) analysis

The ^1H liquid NMR spectrum of DTP which as recorded on a superconducting Fourier transform NMR spectrometer (AVANCE III HD 400, Bruker, Germany). The solid ^{13}C-NMR spectrum of hydrogel was recorded on a superconducting Fourier transform

NMR spectrometer (AVANCE III HD 400, Bruker, Germany).

Self-healing analysis of hydrogel

Macroscopic self-healing experiments were conducted by direct visual inspection and mechanical investigation. The leaf-shaped specimens with reactive red 120 and reactive blue 4 were cut into halves and then the two separate pieces with different color were brought into contact immediately without applied stress. After healing for a certain period, the two pieces of the gel could self-healing automatically at ambient temperature without any other additional stimulus or healing agent. In addition, optical microscopy (OLYMPUS BX51) was used to observe the microscopic changes of cracks in hydrogel with a magnification before and after self-healing.

Hydrogels with 13 mm in diameter and 5 mm in height were cut into two equal parts in the radial direction, and then put them in the original position for self-healing. Self-healing efficiency was determined according to the following formula:

$$\text{Self - healing efficience}\,(\%) = S_h/S_0 \times 100 \qquad (2)$$

where, S_0 and S_h denote the compressive stress of hydrogel before and after self-healing, respectively. Each sample was measured in parallel three times and averaged.

Dual responsive sol–gel transitions of hydrogel

1 g hydrogel prepared by O11 DCMC was demonstrated for the pH responsive sol–gel transitions. The hydrogel was treated with 60 μL HCl (6 mol/L) solution at 60 °C for the gel-to-sol transition. For the sol-to-gel transition, 60 mg Tris was added to neutralize the acid. The same another 1 g hydrogel was demonstrated for the redox responsive sol–gel transitions. To lock the acylhydrazone bonds certain Tris was first added to the hydrogel. 30 mg DTT was added to the hydrogel for for the gel-to-sol transition and 20 μL H_2O_2 were used as the oxidant or the sol-to-gel transition.

Cytotoxicity test of hydrogel

In a clean and airtight centrifugal tube, hydrogels of certain amount freeze-dried were extracted with Dulbecco's modified eagle medium (DMEM) at the concentration of 5 mg/mL for 24 h at 37 °C. The extract was added into serum and double antibodies to prepare DMEM complete medium, that is, high sugar medium consisting of 10% fetal bovine serum (FBS) and 1% double antibodies. Subsequently, L929 cell suspension was seeded on a 96-well plate at a density of 10^5 cells per well. Cells were incubated at 37 °C with 5% CO_2 for 12 h. The cells were washed with sterilized PBS and the culture medium was replaced with the prepared extract. After incubation for 24 h, the medium was removed and cells were washed with PBS. 100 μL complete medium containing 10 μL CCK-8 reagent was added to each medium to incubate for another 24 h. Finally, absorbance at 450 nm was measured by a microplate reader. Cultures in medium without any sample were used as control. Cell viability was calculated by Eq. (3). Samples were made four times in parallel, and the results were expressed by mean and standard deviation.

$$\text{Cell viability}\,(\%) = \frac{A_s - A_0}{A_c - A_0} \times 100 \qquad (3)$$

where, A_0, A_c and A_s denote the absorbance of control group, 10% CCK-8 without cells and sample, respectively.

Mechanical analysis of hydrogel

The mechanical strength of hydrogels was conducted on a universal material testing machine (Instron 5567, USA). For compressive stress, hydrogels were shaped into cylindrical specimens with 13 mm in diameter and 5 mm in height. Hydrogels were cut into rectangular specimens with width of 10 mm and the thickness of 1 mm for tensile stress at the speed of 10 mm/min. Each sample was measured in parallel three times.

The cyclic compression tests were conducted assess the energy dissipation of hydrogels. The consecutive loading–unloading cycles were performed under strain of 60% at a constant stretching rate (60 mm/min). The dissipates energy was calculated as Eq. (4).

$$\Delta U_i = \int_{\text{loading}} \sigma d\varepsilon - \int_{\text{unloading}} \sigma d\varepsilon \qquad (4)$$

where, ΔU_i denotes the dissipated energy for the ith cycle, which is calculated by integrating the area under the stress–strain curve. σ and ε denote stress and strain, respectively.

Results and discussion

DCMC-based dual responsive self-healing hydrogel

Preparation and characterization of hydrogel

The dual-responsive self-healing hydrogel was constructed via acylhydrazone bond and disulfide bond, and the synthetic route of DCMC from CMC is shown in Scheme 1.

In the reaction system, the oxidation of CMC with periodate breaks the C2-C3 bond in the glucose unit in CMC molecule chain. The hydroxyl groups are converted into dialdehyde groups for the attack of I-O bond of the hydroxyl groups of adjacent diols, which is a highly specific selective oxidation reaction without significant side reactions (Li et al. 2011). DCMC with different degrees of oxidation (11.4%, 19.4%, 27.2%), which were coded O_{11}, O_{19} and O_{27} respectively, was generated by using different concentrations of sodium periodate solution and reaction time. During the oxidation, the Mn of DCMCs declined from 1.1×10^6 to 3.7×10^5 with the increase of aldehyde content from 11.8 to 27.2% as shown in Table 1. It is consistent with periodate oxidation mechanism that the opening of glucopyranose ring and the destruction of its ordered packing result in the loss of CMC polymerization degree and higher oxidation correspond to lower Mn (Li et al. 2011).

The formation of dialdehyde groups of DCMC was confirmed by FTIR analysis in Fig. 1a. apparently, there were two characteristic absorption peaks in DCMC, which were located at 1730 cm^{-1} and 886 cm^{-1} regions respectively. The absorption around 1740 cm^{-1} is assigned to aldehydic carbonyl groups, while the infrared band near 886 cm^{-1} is

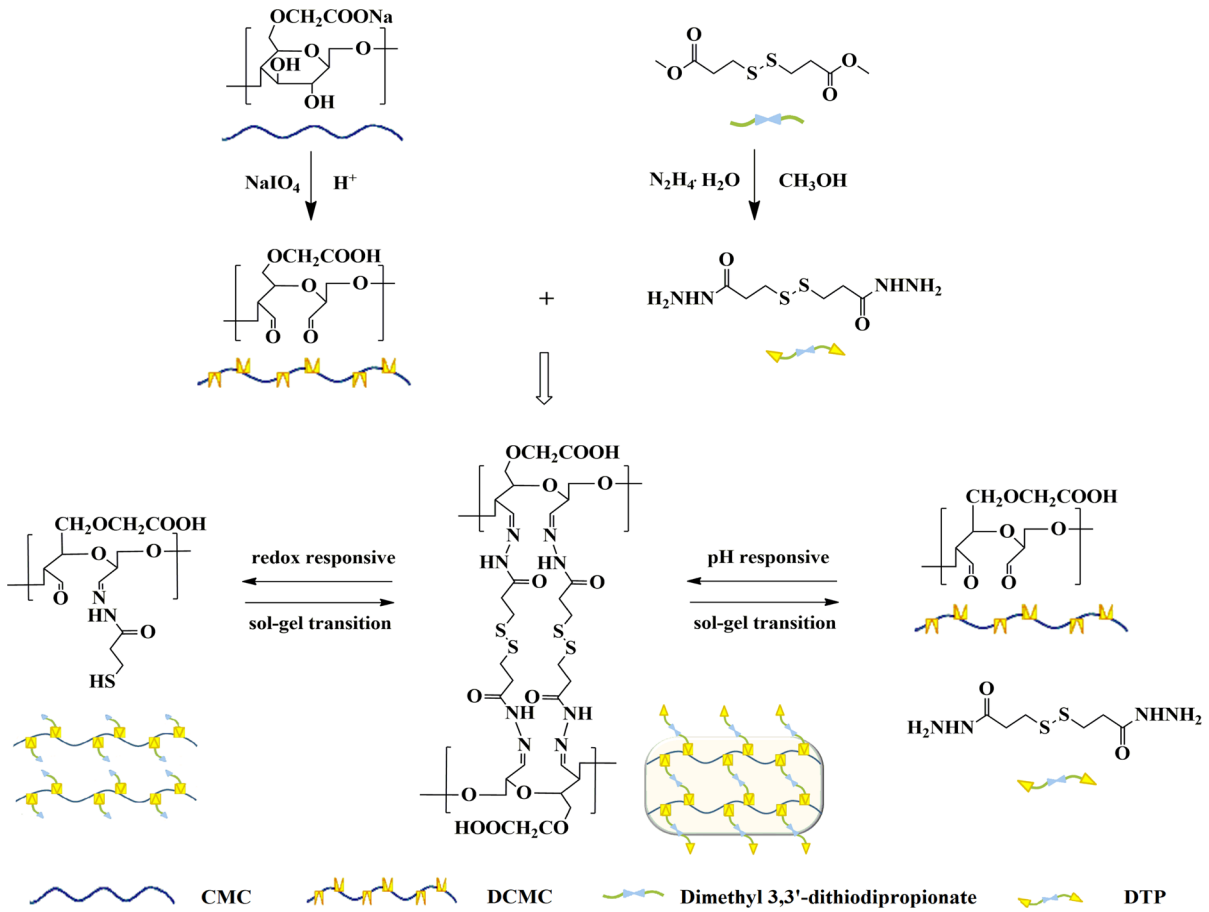

Scheme 1 Strategy for constructing DCMC-based dual responsive self-healing hydrogel and sol–gel transitions

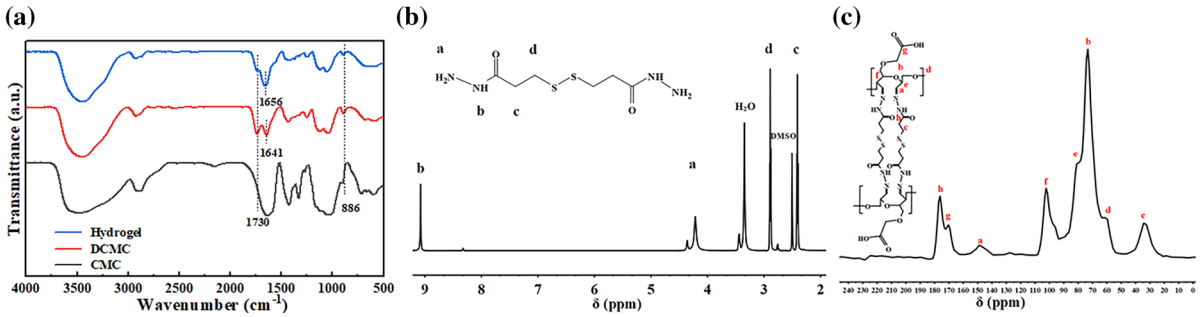

Fig. 1 **a** FTIR spectra of CMC, DCMC and hydrogel. **b** ^{1}H NMR spectrum of DTP. **c** ^{13}C NMR spectrum of hydrogel

characteristic of the formation of hemiacetal bonds (Mu et al. 2012). The results indicated the that aldehyde groups had been successfully introduced into CMC. The formation of hydrogel relied on acylhydrazone covalent bonds according to the infrared spectra in Fig. 1a. The stretching vibration peak at 1730 cm^{-1} attributed to –CHO in DCMC almost disappeared. The characteristic peak of carbonyl group at –CONH at 1641 cm^{-1} shifted to 1656 cm^{-1}, indicating the successful preparation of acylhydrazone-based hydrogel (Shen et al. 2016).

DTP was used widely as an important cross-linker containing hydrazide and disulfide functional groups, which could react with aldehyde groups by Schiff base reactions to from acylhydrazone crosslinking (Wang et al. 2018a). The synthesis scheme of DTP is shown in Scheme 1 and the ^{1}H NMR spectrum is shown in Fig. 1b. The ^{1}H NMR spectra signals appeared around 4.2 ppm is assigned to the NH_2 of acylhydrazine groups. The signal near 9.1 ppm is related to protons of NH near the C=O. In addition, the integral area of the NH_2 of acylhydrazine groups was equal to that of CH_2 near the disulfide bond, which confirmed the successful synthesis of DTP molecular crosslinker.

In addition, Fig. 3c exhibits the ^{13}C NMR spectra of the hydrogel constructed by acylhydrazone bond. The signal at 148 ppm was attributed to the the C=N group of acylhydrazone bond (Monier et al. 2016) which further confirmed the successful crosslinking between DCMC and DTP. The signals at 170, 176 ppm related to the C=O of carboxymethyl on DCMC and acylhydrazone bond, respectively. The signals at 61,73, 81, 96, 102 ppm presented other carbons of DCMC and the signal at 34 ppm was is assigned to CH_2 of DTP.

Factors on formation of self-healing hydrogel

It is necessary to control the appropriate gelation time in order to avoid gel inhomogeneity resulting from rapid gelation and time wasting for the gelling process. The effects of weak acid concentration, gelator concentration and degree of oxidation on hydrogel gelation time were discussed. Hydrogels with different gelator concentrations were prepared by O_{19} DCMC at pH of 3.5, 4, 5 and 6. As shown in Fig. 2a, when the gelator increased from 6 to 10%, the gelation time decreased from dozens of seconds to seconds at pH of 3.5 and decreased from 1600 s to less than 500 s at pH of 6.0. It indicated that increasing percentage of the solid in hydrogel provided more chances to crosslink acylhydrazine with aldehydes resulting in faster formation of acylhydrazone bond. Furthermore, when the gelator concentration was fixed, the gelation time of hydrogel was increased from a few seconds to thousands of seconds with increment of pH value from 3.5 to 6.0. This phenomenon can be explained by the formation mechanism of acylhydrazone bond that carbonyl oxygen in weak acidic environment is easier to protonate and the protonated carbonyl is easier to bond with DTP hydrazide groups, thus accelerating the formation of acylhydrazone bond (Liu et al. 2012; Sun et al. 2018). In order to explore the effect of the oxidation degree of DCMC on the preparation of DCMC-based hydrogels, hydrogels with a concentration of 8% were prepared with DCMC with different oxidation degrees under four different pH conditions of 3.5,4.0,4.5 and 5.0. In Fig. 2b, it is obvious that the higher oxidation degree of DCMC shorten the gelation time at the same pH and gelator concentration. The reasonable explanation is that in the DCMC-based hydrogel with the same gelator factor concentration,

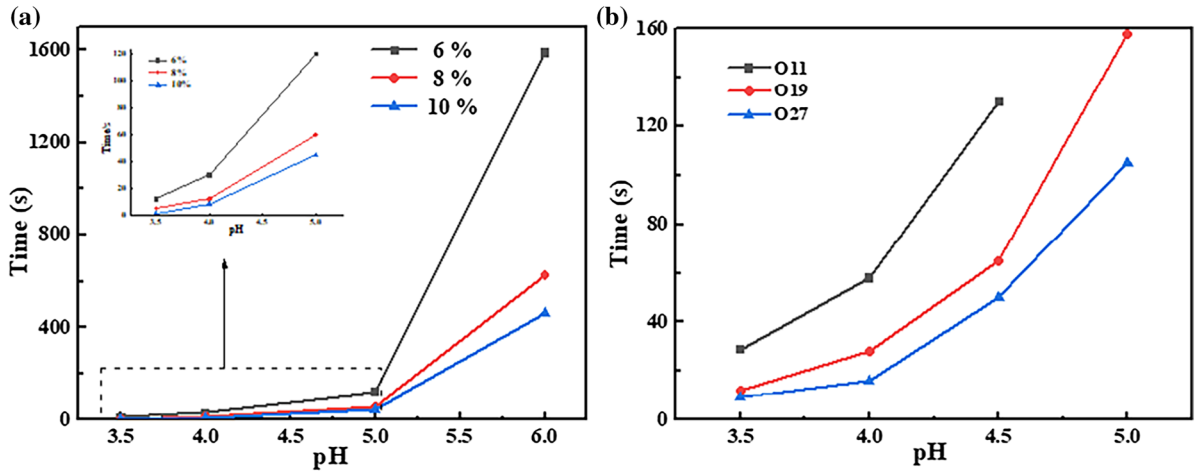

Fig. 2 Effects of **a** pH, gelator concentration and **b** oxidation degree of DCMC on formation of DCMC-based hydrogel

the higher oxidation degree of DCMC contains more aldehyde groups which react with DTP hydrazide groups. Therefore, the DCMC-based hydrogel with higher oxidation degree of DCMC fabricated faster when the pH and gel factor concentration were the same.

Performances of the self-healing hydrogels

The self-healing behaviour of DCMC-based hydrogel could be observed directly. As shown in Fig. 3a, two leaf hydrogels stained with reactive red 120 and reactive blue 4 were cut in halves respectively. Subsequently, two different coloured half leaf gels were intimately contacted along the cutting line without any external interference at room temperature. Two lobular hydrogels stained with reactive red 120 and reactive blue 4 narrowed the fissure after 1 h and could fully combined into a complete hydrogel after 6 h. In addition, the optical microscopic image in Fig. 3b clearly shows the self-healing process of the hydrogel. The crack caused by the bistoury gradually healed after 1 h without any external force at room temperature, and disappeared after 6 h, which also confirmed the existence of self-healing phenomenon. As schematically illustrated in Fig. 3c, DCMC-based hydrogels to maintain their integrity while exhibiting excellent network rearrangement capabilities through rapidly breaking and reforming of the reversible acylhydrazone linkages.

Due to the dynamic acylhydrazone and disulfide bonds (Liu et al. 2017a), DCMC-based hydrogel also has interesting sol–gel transitions which present the stimuli-responsibility of hydrogels (Deng et al. 2010). Hydrogels were prepared by O_{11} DCMC at weak acid to display the dual responsive sol–gel transitions as shown in Fig. 4a. The hydrogel was completely dissolved into liquid after being treated with hydrochloric acid solution (60 µL, 6 mol/L) at 60 °C. However, when Tris was added to neutralize acid, the solution returned to the gel state. Tris was added to avoid toxicity and irritant smell of three ethylamine which were usually to be chosen (Du et al. 2019; Hussain et al. 2018b). The pH response of DCMC-based self-healing hydrogel to sol–gel transition is essentially the reaction process of acylhydrazone bond to pH. As depicted in Scheme 1, the addition of strong acid promotes the reverse reaction and the hydrogel decomposes as raw material, while the strong acid is neutralized, positive reaction promotes the hydrogel formation.

The disulfide bonds in DCMC-based self-healing hydrogel can undergo redox reaction (Hou et al. 2018). The disulfide bond is a weak reversible covalent bond, which can be reduced to sulfhydryl group under the action of reducing agent and the sulfhydryl group can be oxidized to disulfide bond after the addition of oxidant (Li et al. 2016). The exchange reaction of disulfide bonds can be promoted under alkaline conditions and inhibited under acidic conditions (Du

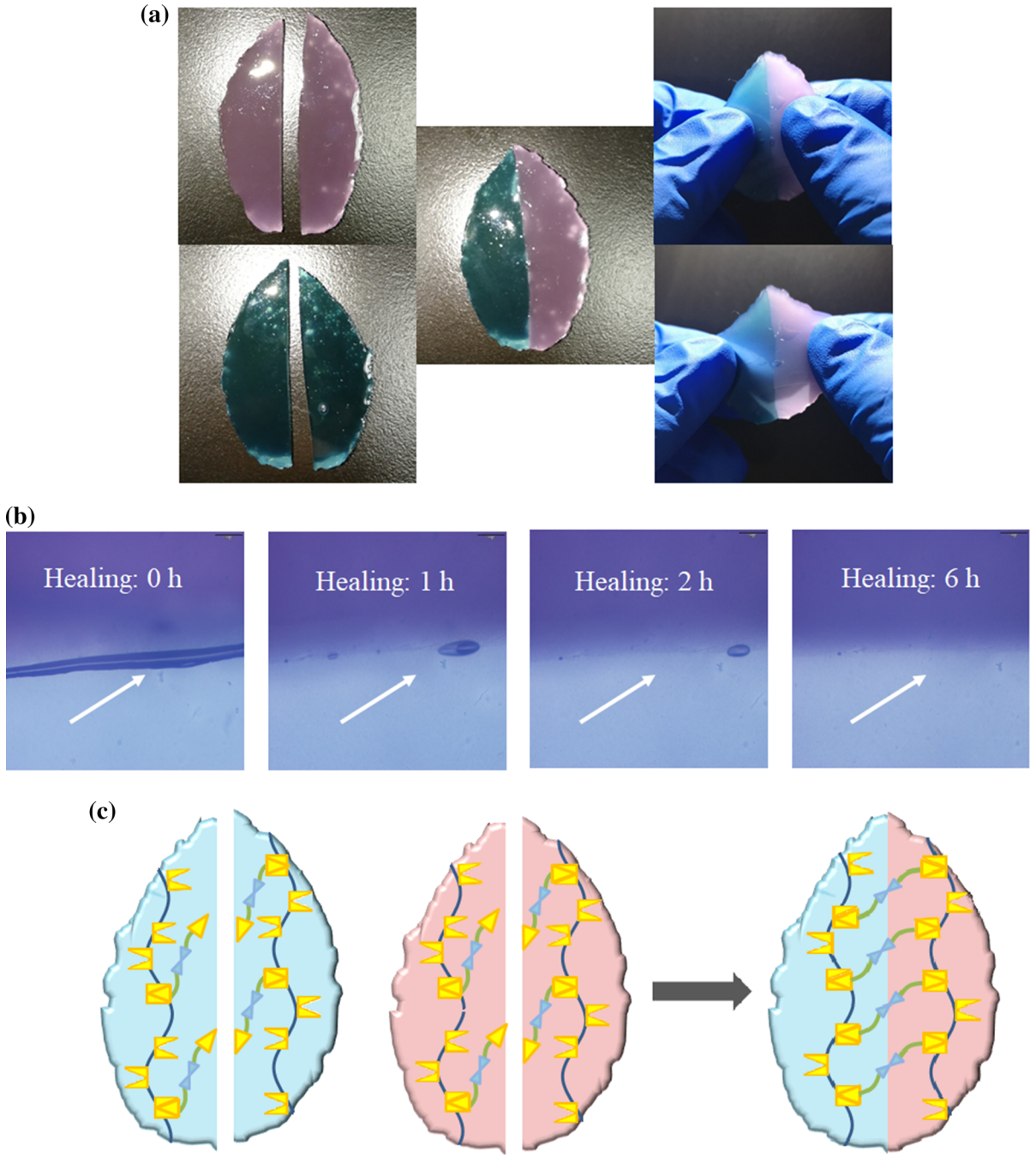

Fig. 3 Macroscopic (**a**) and microscopic (**b**) images of DCMC-based hydrogels (8%) before and after self-healing process. **c** Schematic illustration for the dynamic hydrogel networks through self-healing process

et al. 2019). We add Tris into the gel to ensure the closure of the acylhydrazone bond. Hydrogel shows reversible sol–gel transition behavior under redox conditions in Fig. 4b. Hydrogel dissolves into solution because of the addition of reductant DL-Dithiothreitol (DTT) and the hydrogel regenerates again after adding oxidant H_2O_2. It is illustrated in Scheme 1 that the covalent disulfide bond is easy to break into thiol group under reduction condition, and then regenerate under oxidation condition (Li et al. 2016).

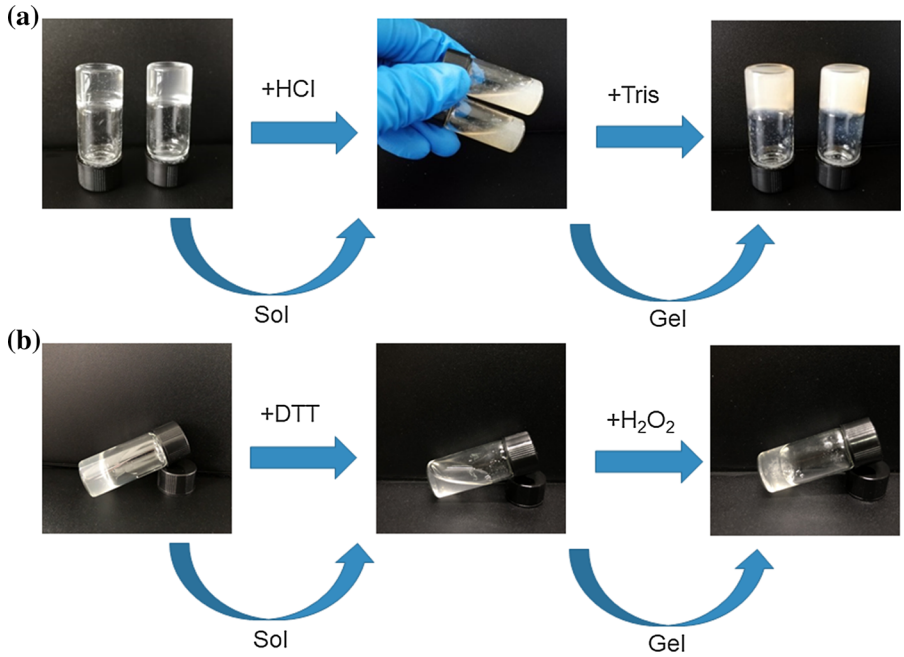

Fig. 4 Sol–gel transitions of DCMC-based hydrogel in response to pH and redox triggers. The concentration of all the samples was 8%

DCMC was reported to effectively crosslink free amino groups inside of porcine arteries. The residual free aldehyde groups were suspected to create a locally cytotoxic environment in arteries (Shao et al. 2017; Wang et al. 2016). In order to determine whether the DCMC-based self-healing hydrogels have good biocompatibility with tissues and cells, cytotoxicity tests were carried out on hydrogels with different degrees of oxidation. The extract of freeze-dried DCMC-based self-healing gel with different oxidation degrees were added with serum and double antibody to prepare DMEM complete medium. Then L929 cell suspension was inoculated on the density plate, and cells were cultured under certain conditions for 24 h. The cell viability was detected by enzyme labelling instrument to detect the cytotoxicity of DCMC-based hydrogels and was calculated according to relevant formulas. The cell viabilities of hydrogels with O_{11}, O_{19} and O_{27} DCMC shown in Fig. 5 indicated that DCMC-based self-healing hydrogels had good biocompatibility. High activity and effective proliferation of L929 cells in hydrogels may be due to their good biocompatibility and reversible cross-linking network of DCMC-based hydrogels. These results indicate that hydrogels have potential application prospects in biomedical applications.

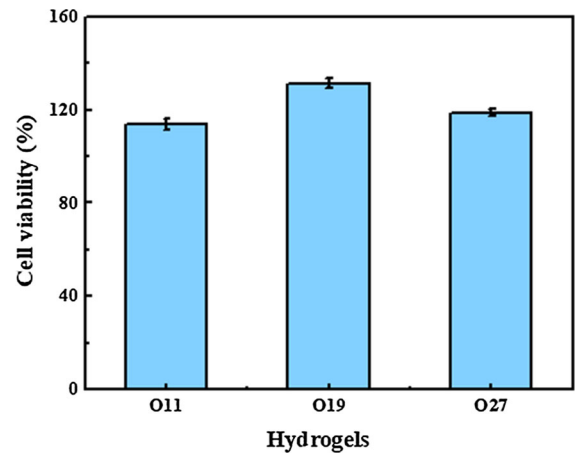

Fig. 5 Cell viability of hydrogels (8%) with different degrees of oxidation

Effects of CNFs on self-healing hydrogels

Effects of CNFs on mechanical property

In order to examine the effect of CNFs on the mechanical strength and toughness, CNFs nanocomposite hydrogels with different CNFs content were prepared. As shown in Fig. 6a, the original DCMC-based hydrogel without CNFs exhibits good toughness

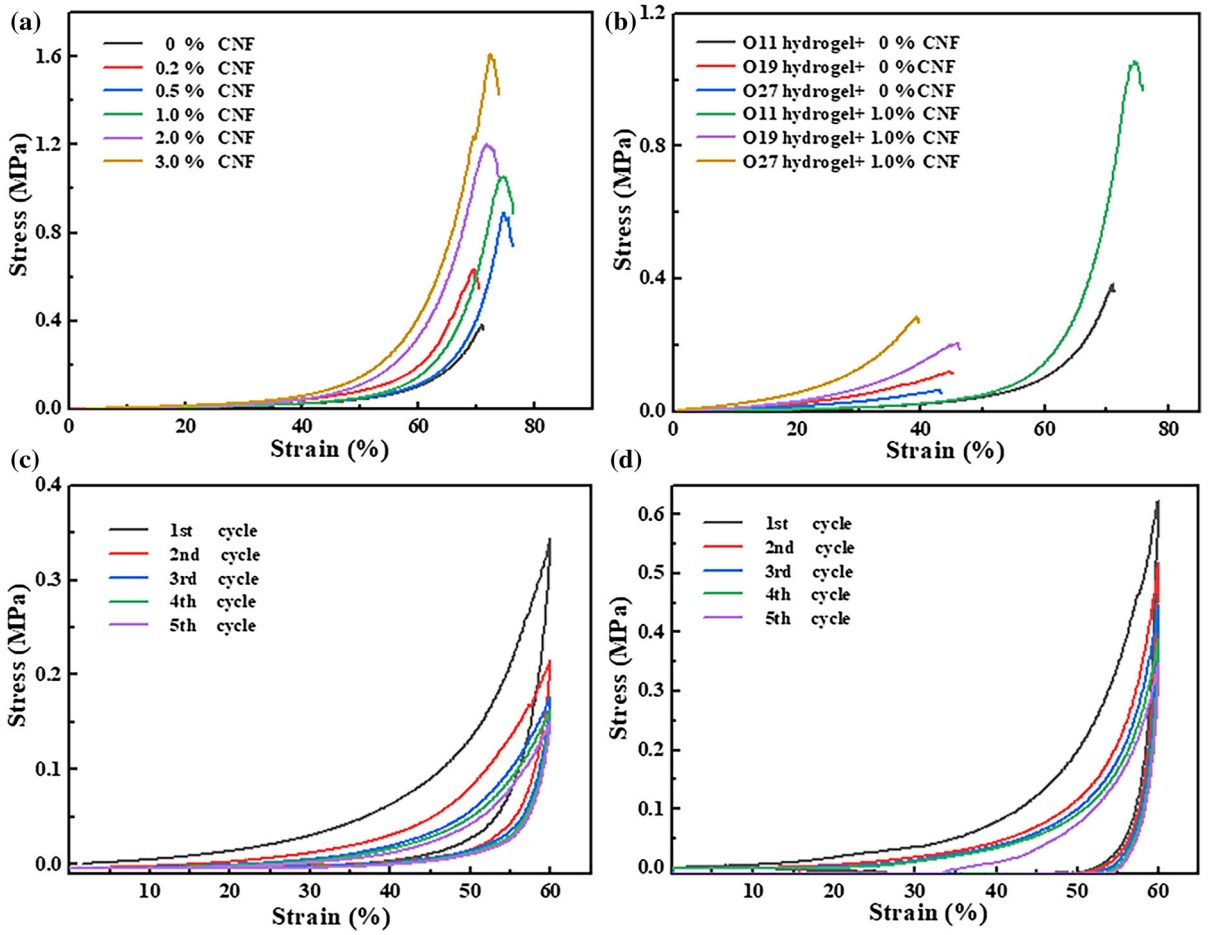

Fig. 6 Compressive stress–strain curves of hydrogels **a** under different content of CNFs and **b** with different degrees of oxidation; cyclic compress five successive loading–unloading curves at 60% strain of **c** O11 hydrogel and **d** O11 hydrogel with 1.0 wt% CNFs. The concentration of all of the samples was 8%

(strain 70.9%) and weaker mechanical strength (0.38 MPa). With the augment of CNFs content in the hydrogels, the compressive strength of the hydrogels increased gradually. When the CNFs content was less than 1.0 wt%, the stress and strain of the hydrogel were higher than that of the original hydrogel. Mechanical strain of hydrogel reached 74.7% when the content of CNFs was 1.0 wt% and the mechanical strength was 1.05 MPa, which were 1.06- and 2.76-fold higher than those of pristine DCMC-based hydrogel. However, when the content of CNFs continues to increase, the stress of the gel continues to increase, but the strain decreases. The mechanical strength of hydrogel with 3.0 wt% CNFs run up to 1.61 MPa with certain decrease in breaking stress. Similar results were found in the research that CNFs were added to PAA hydrogels to improve the mechanical strength and toughness of PAA hydrogels by Shao et al. (Shao et al. 2017). They attributed the increase in mechanical reinforcement to the addition of well-dispersed rigid CNFs fillers to resist stress concentration and transfer energy through the interface to prevent crack propagation. In the DCMC-based hydrogel system, the reasonable explanation is that the addition of rigid CNFs resist stress concentration and transfer the energy through the interface via hydrogen bond between CNFs and DCMC to prevent crack propagation, which is supported by the increased gel content observed at CNFs concentrations up to and including 1.0 wt%. While at increased CNFs loadings of 2.0 wt% and 3.0 wt%, the rigidity of the hydrogel increases and the toughness decreases. A probable

reason for this reduction in mechanical behavior is the large volume of CNFs preventing effective crosslinking formation between DCMC and DTP, which is more crucial than the hydrogen bonds between CNFs and DCMC contribute towards the mechanical behavior of the hydrogels (Wang et al. 2017).

Uniaxial compressive tests of DCMC-based hydrogels with different degrees of oxidation and 1.0 wt% CNFs hydrogels were measured to investigate the mechanical properties of DCMC-based hydrogels with different degrees of oxidation. As shown in Fig. 6b, strength and strain of hydrogel with O_{11} DCMC were larger than that of hydrogels prepared by O_{19} and O_{27}, and the compressive strength of hydrogels decreases with the increase of oxidation degree of DCMC. When 1.0 wt% CNF was added, the fracture stress of the three kinds of DCMCs-based hydrogels increased. The strain of O_{11} and O_{19} hydrogels increases with the addition of 1.0 wt% CNFs, while the strain of O_{27} hydrogels decreases. The reasonable explanation is that the DCMCs with a higher degree of oxidation have relatively shorter molecular chains, which increased entanglement of DCMC molecular chains and reduced the toughness of hydrogels (Shao et al. 2017).

To further confirm that 1.0 wt% CNFs is beneficial to mechanical property, DCMC-based hydrogel with 1.0 wt% CNFs and the original hydrogel were prepared into cylinders with 13 mm in diameter and 5 mm in height to investigate the hysteresis behavior during the successive loading–unloading cycle. It could reflect the energy dissipation of hydrogel samples, which was an indicator to assess the toughness of the sample (Spoljaric et al. 2014). As can be seen from Fig. 6c, d, the cycle diagrams of the self-healing hydrogel with 1.0 wt% CNFs are tighter than that of the hydrogel without CNFs. Integrating the closed curve of each cycle, the dissipated energy of the hydrogels of each cycle was obtained in Table 2. After five uniaxial successive loading–unloading, the stress at 60% strain of the DCMC-based self-healing hydrogel was 0.15 MPa which remains 43.8% of that of the first cycle (0.34 MPa). While the stress at 60% strain of the DCMC-based self-healing hydrogel with 1.0 wt% CNFs was 0.35 MPa which accounted 56.1%. The results of cyclic compress five successive loading–unloading curves at 60% strain and the energy dissipation data illustrated that the DCMC-based self-healing hydrogel with 1.0 wt% CNFs dissipated energy relatively slowly, which further verified the existence of sacrificial bonds from hydrogen bond between CNFs and carboxyl groups of DCMC.

Table 2 The dissipated energy of the hydrogels without and with 1.0 wt% CNFs of each cycle

Cycle index	△U (kJ/m^3)	
	+ 0% CNFs	+ 1.0 wt% CNFs
1	2.82	5.29
2	1.56	3.27
3	1.02	3.03
4	0.92	2.83
5	0.78	1.91

Effects of CNFs on sol–gel transition and self-healing property

In addition, the effect of CNFs on the mechanical strength of DCMC-based self-healing hydrogel was also studied before and after sol–gel transition. Hydrogels of 8% gelator concentration were shaped into 50 mm in length and 10 mm wide slices with a thickness of 2 mm to conduct the uniaxial tensile test. Tensile stress–strain curves in Fig. 7 show that the tensile strength of DCMC-based self-healing hydrogel containing 1.0 wt% CNFs is 25.3 kPa more than twice 12.2 kPa of hydrogel without CNFs and the increase in strain, which further confirmed that CNFs could resist

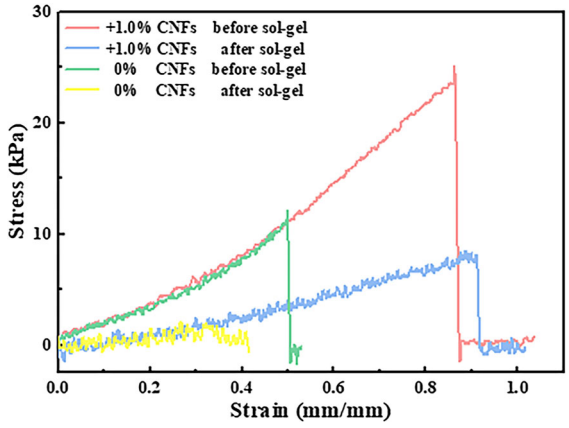

Fig. 7 Tensile stress–strain curves of hydrogels before and after sol–gel transition of redox triggers. The concentration of all the samples was 8%

stress concentration to prevent crack propagation. Moreover, DCMC-based self-healing hydrogel containing 1.0 wt% CNFs still had a certain tensile strength after completion of first redox sol–gel transition, which was about 34.3% of original value. However, the original self-healing hydrogel has little or even no tensile strength after sol–gel transition, which has been just in accord with the report that the cycle index of gel–sol transition is limited and for the lower gelator concentration (< 10%), the hydrogel can be repeated only twice (Hussain et al. 2018b). DCMC-based hydrogel added with CNFs seems to be more resistant to destruction of hydrogel structure by sol–gel process.

DCMC-based self-healing hydrogels with different CNFs content were prepared and tested under a tensile test machine to explore whether CNFs have an effect on the self-healing behaviors of hydrogels. The hydrogels were cut into two sections with a scalpel and the incision were aligned in an airtight container without any external conditions to heal themselves. The original tensile strength of the hydrogel and the hydrogels after self-healing for 0.5 h and 1 h were tested respectively. The self-healing efficiency was calculated by using the relevant formulas. Figure 8 shows that when the hydrogels self-healed for 0.5 h, the self-healing efficiency without CNFs was 51.6%, while that of hydrogels with 0.5 wt% was 69.2% and with 1.0 wt% CNFs was 82.7%, respectively. When the hydrogel self-healed for 1 h, the self-healing efficiency of the hydrogel without CNFs was 58.5%, while that of the 0.5 wt% hydrogel was 82.4%, and that of the 1.0 wt% CNFs was 89.9%. In other words, the self-healing efficiency of CNFs composite self-healing hydrogels increased gradually with the increase of CNFs content (within 1.0 wt%) in the same self-healing time. It can be reasonably explained that when the gel factor concentration is relatively low, at the gel wound interface, the CNFs bond promotes the formation of hydrogen bonds at the same time as the acylhydrazone bonds recombine (Wang et al. 2017). Then the hydrogel with 0.5 wt% and 1.0 wt% CNFs restored faster than the original DCMC-based self-healing hydrogel.

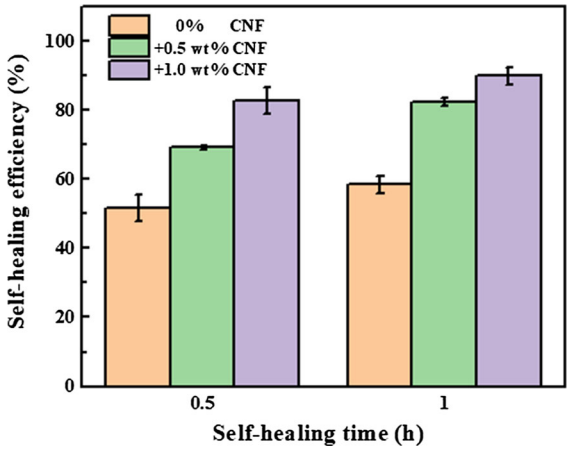

Fig. 8 Self-healing efficiency of hydrogels (8%) with different content of CNFs

Conclusions

A self-healing hydrogel without cytotoxicity was successfully prepared via the crosslinking of DCMC and DTP through constructing arylhydrazone bond. The DCMC-based self-healing hydrogel contains hydrazide bond and disulfide bond with pH response and redox reaction. The decrease of pH and the increase of gelator concentration and DCMC oxidation degree accelerated the formation of hydrogel and the formation velocity of hydrogels could be regulated simply by the above three factors during preparation. Furthermore, CNFs with less than 1.0 wt% content improved the mechanical property with compressive strength of 1.15 MPa and strain 74.6% DCMC-based self-healing hydrogel and helped to maintain certain mechanical strength after sol–gel. While 2.0 wt% and 3.0 wt% CNFs only increased the compressive strength of hydrogels, but the strain of hydrogels decreased due to the superfluous rigidity of CNFs. The mechanical properties of self-healing hydrogels can be improved and controlled by adding CNFs to meet special requirements for mechanical properties and to regulate self-healing efficiency.

Acknowledgments This work was supported by the Science and Technology Program of Guangzhou (201607020025), the National Natural Science Foundation of China (31570569), National Key R&D Program of China (2017YFD0601003) and the foundation of State Key Laboratory of Pulp and Paper Engineering (2017QN01; 2018PY01).

References

Abe K, Yano H (2012) Cellulose nanofiber-based hydrogels with high mechanical strength. Cellulose 19:1907–1912

Chen Y et al (2018) A thermo-/pH-responsive hydrogel (PNIPAM-PDMA-PAA) with diverse nanostructures and gel behaviors as a general drug carrier for drug release. Polym Chem UK 9:4063–4072

Deng GH, Tang CM, Li FY, Jiang HF, Chen YM (2010) Covalent cross-linked polymer gels with reversible sol–gel transition and self-healing properties. Macromolecules 43:1191–1194

Deng GH et al (2012) Dynamic hydrogels with an environmental adaptive self-healing ability and dual responsive sol–gel transitions. ACS Macro Lett 1:275–279

Du JH, Choi B, Liu YX, Feng AC, Thang SH (2019) Degradable pH and redox dual responsive nanoparticles for efficient covalent drug delivery. Polym Chem UK 10:1291–1298

Guo RW, Su Q, Zhang JW, Dong AJ, Lin CG, Zhang JH (2017) Facile access to multisensitive and self-healing hydrogels with reversible and dynamic boronic ester and disulfide linkages. Biomacromolecules 18:1356–1364

Hou XB, Li YC, Pan YF, Jin YC, Xiao HM (2018) Controlled release of agrochemicals and heavy metal ion capture dual-functional redox-responsive hydrogel for soil remediation. Chem Commun 54:13714–13717

Hussain I, Sayed SM, Liu SL, Oderinde O, Kang MM, Yao F, Fu GD (2018a) Enhancing the mechanical properties and self-healing efficiency of hydroxyethyl cellulose-based conductive hydrogels via supramolecular interactions. Eur Polym J 105:85–94

Hussain I, Sayed SM, Liu SL, Yao F, Oderinde O, Fu GD (2018b) Hydroxyethyl cellulose-based self-healing hydrogels with enhanced mechanical properties via metal-ligand bond interactions. Eur Polym J 100:219–227

Li HL, Wu B, Mu CD, Lin W (2011) Concomitant degradation in periodate oxidation of carboxymethyl cellulose. Carbohydr Polym 84:881–886

Li DF, Ye YX, Li DR, Li XY, Mu CD (2016) Biological properties of dialdehyde carboxymethyl cellulose crosslinked gelatin-PEG composite hydrogel fibers for wound dressings. Carbohydr Polym 137:508–514

Liu FY, Li FY, Deng GH, Chen YM, Zhang BQ, Zhang J, Liu CY (2012) Rheological images of dynamic covalent polymer networks and mechanisms behind mechanical and self-healing properties. Macromolecules 45:1636–1645

Liu HC, Sui XF, Xu H, Zhang LP, Zhong Y, Mao ZP (2016) Self-healing polysaccharide hydrogel based on dynamic covalent enamine bonds. Macromol Mater Eng 301: 725–732

Liu HC et al (2017a) Facile fabrication of redox/pH dual stimuli responsive cellulose hydrogel. Carbohydr Polym 176: 299–306

Liu YJ, Cao WT, Ma MG, Wan PB (2017b) Ultrasensitive wearable soft strain sensors of conductive, self-healing, and elastic hydrogels with synergistic "soft and hard" hybrid networks. ACS Appl Mater Interfaces 9:25559–25570

Liu HC et al (2018) Self-healing and injectable polysaccharide hydrogels with tunable mechanical properties. Cellulose 25:559–571

Maity S, Parshi N, Prodhan C, Chaudhuri K, Ganguly J (2018) Characterization of a fluorescent hydrogel synthesized using chitosan, polyvinyl alcohol and 9-anthraldehyde for the selective detection and discrimination of trace Fe^{3+} and Fe^{2+} in water for live-cell imaging. Carbohydr Polym 193:119–128

Monier M, Abdel-Latif DA, Ji HF (2016) Synthesis and application of photo-active carboxymethyl cellulose derivatives. React Funct Polym 102:137–146

Mu CD, Guo JM, Li XY, Lin W, Li DF (2012) Preparation and properties of dialdehyde carboxymethyl cellulose cross-linked gelatin edible films. Food Hydrocolloids 27:22–29

Peng YY, Duan CY, Elias R, Lucia LA, Fu SY (2019) A new protocol for efficient and high yield preparation of cellulose nanofibrils. Cellulose 26:877–887

Rodriguez-Docampo Z, Otto S (2008) Orthogonal or simultaneous use of disulfide and hydrazone exchange in dynamic covalent chemistry in aqueous solution. Chem Commun 42:5301–5303

Shao CY, Chang HL, Wang M, Xu F, Yang J (2017) High-strength, tough, and self-healing nanocomposite physical hydrogels based on the synergistic effects of dynamic hydrogen bond and dual coordination bonds. ACS Appl Mater Interfaces 9:28305–28318

Shen YQ et al (2016) pH and redox dual stimuli-responsive injectable hydrogels based on carboxymethyl cellulose derivatives. Macromol Res 24:602–608

Spoljaric S, Salminen A, Luong ND, Seppala J (2014) Stable, self-healing hydrogels from nanofibrillated cellulose, poly(vinyl alcohol) and borax via reversible crosslinking. Eur Polym J 56:105–117

Sun PP, Ren SJ, Liu FL, Wu AL, Sun N, Shi LJ, Zheng LQ (2018) Smart low molecular weight hydrogels with dynamic covalent skeletons. Soft Matter 14:6678–6683

Tian XZ, Jiang X (2018) Preparing water-soluble 2,3-dialdehyde cellulose as a bio-origin cross-linker of chitosan. Cellulose 25:987–998

Wang X, Tang P, Xu YW, Yang X, Yu XX (2016) In vitro study of strontium doped calcium polyphosphate-modified arteries fixed by dialdehyde carboxymethyl cellulose for vascular scaffolds. Int J Biol Macromol 93:1583–1590

Wang YX, Wang ZC, Wu KL, Wu JN, Meng GH, Liu ZY, Guo XH (2017) Synthesis of cellulose-based double-network hydrogels demonstrating high strength, self-healing, and antibacterial properties. Carbohydr Polym 168:112–120

Wang L, Zhou WF, Wang QG, Xu C, Tang Q, Yang H (2018a) An injectable, dual responsive, and self-healing hydrogel based on oxidized sodium alginate and hydrazide-modified poly(ethyleneglycol). Molecules 23:1–12

Wang WD, Narain R, Zeng HB (2018b) rational design of self-healing tough hydrogels: a mini review. Front Chem 6:1–9

Wei Z et al (2015) novel biocompatible polysaccharide-based self-healing hydrogel. Adv Funct Mater 25:1352–1359

Xu J, Yang DG, Li WJ, Gao Y, Chen HB, Li HM (2011) Phenylboronate-diol crosslinked polymer gels with reversible sol-gel transition. Polymer 52:4268–4276

Yang J, Han CR, Duan JF, Ma MG, Zhang XM, Xu F, Sun RC (2013) Synthesis and characterization of mechanically flexible and tough cellulose nanocrystals-polyacrylamide nanocomposite hydrogels. Cellulose 20:227–237

Yang XP, Abe K, Biswas SK, Yano H (2018a) Extremely stiff and strong nanocomposite hydrogels with stretchable cellulose nanofiber/poly(vinyl alcohol) networks. Cellulose 25:6571–6580

Yang Y, Zhu HK, Wang J, Fang Q, Peng ZP (2018b) Enzymatically disulfide-crosslinked chitosan/hyaluronic acid layer-by-layer self-assembled microcapsules for redox-responsive controlled release of protein. ACS Appl Mater Interfaces 10:33493–33506

Yu F, Cao XD, Li YL, Zeng L, Yuan B, Chen XF (2014) An injectable hyaluronic acid/PEG hydrogel for cartilage tissue engineering formed by integrating enzymatic crosslinking and Diels–Alder "click chemistry". Polym Chem UK 5:1082–1090

Yu F, Cao XD, Du J, Wang G, Chen XF (2015) Multifunctional hydrogel with good structure integrity, self-healing, and tissue-adhesive property formed by combining die is Alder click reaction and acylhydrazone bond. Acs Appl Mater Interfaces 7:24023–24031

Zhu CY et al (2017) A hydrogel-based localized release of colistin for antimicrobial treatment of burn wound infection. Macromol Biosci 168:112–120